Journal of Marine Research, 50, 183–205, 1992

Journal of
MARINE RESEARCH

Volume 50, Number 2

The stability of a canonical front

by John Kroll[1]

ABSTRACT

The stability of a geostrophic frontal current of constant slope over a stratified ocean is investigated using asymptotic techniques for large horizontal wavenumber and a small Burger number. The front is called canonical because it should approximate the edges of eddies or boundary currents. Results show that the front is unstable for an along the front wavenumber greater than f/V_0 where V_0 is the current velocity. But the instability is confined to a region near the vertex of the front of horizontal extent $0(V_0/f)$. The flow becomes more unstable for increasing wavenumber and it is speculated that this region near the vertex will be strongly mixed, rounding off the sharp vertex of the steady state flow. There will be strong internal wave propagation from the interface of this region into the ocean when the frequency is greater than f.

1. Introduction

In the past, eddies and fronts in the ocean and atmosphere have been studied using the quasi-geostrophic approximation where the time dependent terms and nonlinear terms in the equations of motion are assumed small compared to the basic geostrophic balance. Examples of its use are Hoskins and Bretherton (1972) for fronts and McWilliams and Flierl (1976) for eddies. However, in many cases the necessary condition for its use, that the Rossby number, ϵ, be much less than unity, is not fulfilled. For example, the typical isolated eddy has $\epsilon \simeq 1/4$ (Joyce, 1984) where ϵ is defined as the ratio of the absolute value of the angular swirl speed to the Coriolis parameter. This is not a small ϵ, and also, the eddy has a significant density jump

1. Department of Mathematics and Statistics, Old Dominion University, Norfolk, Virginia, 23529, U.S.A.

across its sloping interface with the surrounding water which cannot be handled by standard quasi-geostrophic dynamics.

More recently the "reduced gravity" or "1.5 layer" model has been used. This consists of an active homogeneous layer of inviscid fluid over an inactive homogeneous layer of higher density and infinite depth. The aspect ratio of depth to horizontal scale in the top layer is assumed small and the time dependence and nonlinear effect are order one.

This model was first applied to fronts by Griffiths *et al.* (1982) and showed that instabilities can exist. Subsequently, Killworth and Stern (1982) applied it to a density driven boundary current and found the flow can be unstable for a mean potential vorticity increasing toward the boundary and the mean current vanishing at the boundary. At about the same time Paldor (1983) applied it to essentially the same type of current but with uniform potential vorticity and found the flow to be stable. Cushman-Roisin (1986a) assumed a time scale much larger than inertial and derived a model which might be characterized as a combination of the quasi-geostrophic and 1.5 layer models which can deal with situations where the interface slopes are important.

The 1.5 layer model was first applied to eddies by Cushman-Roisin *et al.* (1985). Actually, the application to eddies goes back to the problem of a rotating fluid with a varying elliptical bounding surface. That nonlinear problem has a long history (see Lamb (1945), Chap. 12). It was found that solutions to it can be found in a form separable in time and horizontal space with the equation in horizontal space in the form of a polynomial. Later, Ball (1963) found integral constants of the motion. The long wave shallow water equations used for that problem are the same as those that result from the 1.5 layer model. This was exploited by Cushman-Roisin *et al.* (1985) to identify and investigate two special cases of the general solution applicable to oceanic eddies. One was the "rodon" solution in which an ellipsoid of constant size rotated uniformly anticyclonically. The other was an axisymmetric anticyclonic vortex with an oscillating horizontal divergence (later called the "pulson" solution by Kirwan and Liu (1988)). Subsequently, Young (1986) classified the general vortex solutions in size, shape and orientation with changes in size being at the inertial frequency, changes in shape superinertial, and changes in orientation being either sub or superinertial. Cushman-Roisin (1987) found an exact solution to a combined pulson-radon case. Cushman-Roisin (1986b) and Ripa (1987) investigated the stability of the general rodon case and showed that instabilities occur if the eccentricity of the eddy is sufficiently large. They also showed that the normal modes of the perturbation of these cases will be a function of finite degree polynomials. Kirwan and Liu (1988) investigated the general separable solutions for a wide range of conditions. These conditions were not confined to what are considered realistic for oceanic application.

The next logical step in modelling a more realistic eddy or front is to add a stratified interior. We are not only interested in the influence of this additional effect

on stability but also in the character of the internal waves that could be generated. Our investigation began with an investigation of a circular eddy. It became apparent, however, that it was the dynamics occurring at the edge which were most important. So it was decided to study a front of constant slope first.

Some previous work may indicate what we should expect. Kroll (1982, 1988) investigated the stability of a mixed layer that included a mean flow over a stratified ocean separated by a density jump interface. The main difference with the present study was that the interface had no slope. Results from that study indicated an instability for wave perturbations in the direction of the mean flow. So we might expect an unstable wave in the direction of the mean frontal current no matter how the mean potential vorticity varies.

The front investigated here has a constant slope and should be about as simple as is possible while still retaining the essential physics. The results, at least to some degree, should apply to any front or eddy edge where the curvature of the front is sufficiently small over the scale of interest. Hence we call this front "canonical."

2. Formulation of model

We consider a frontal current in a layer with depth $h(y)$ and uniform density ρ_1 which overlays an infinitely deep stratified ocean with density $\rho_2(z) > \rho_1$. We will designate the top layer as the "current" and bottom layer as the "ocean."

We assume the system on an f-plane and that the surface acts like a rigid lid. In the current we have the usual shallow water (nonlinear) equations. In the ocean we assume no heat conduction, density perturbations sufficiently small to use the Bousinesq approximation, a linear equation of state, motions sufficiently small that nonlinear terms can be neglected and vertical scales of motion much less than that of the horizontal. The equations of motion are then:

For the current:

$$\begin{aligned} u_{1t} + u_1 u_{1x} + v_1 u_{1y} - f v_1 &= -\frac{1}{\rho_1} p_{1x} \\ v_{1t} + u_1 v_{1x} + v_1 v_{1y} + f u_1 &= -\frac{1}{\rho_1} p_{1y} \\ u_{1x} + v_{1y} + w_{1z} &= 0. \end{aligned} \tag{1}$$

For the ocean

$$\begin{aligned} u_{2t} - f v_2 &= \frac{-1}{\rho_1}\left[p_{2x} - g(\bar{\rho}_2(-h) - \rho_1)h_x\right] \\ v_{2t} + f u_2 &= \frac{-1}{\rho_1}\left[p_{2y} - g(\bar{\rho}_2(-h) - \rho_1)h_y\right] \\ p_{2_{zt}} &= g w_2 \bar{\rho}_{2z} \\ u_{2x} + v_{2y} + w_{2z} &= 0 \end{aligned} \tag{2}$$

where $\bar{\rho}_2(z)$ is the density of the basic state in the ocean and the reference density ρ_1 is assumed constant. The boundary and interface conditions are for the current:

$$\text{at} \qquad z = 0, w_1 = 0$$
$$\text{at} \qquad z = -h(x, y, t), h_t + u_1 h_x + v_1 h_y = -w_1$$

and for the ocean:

$$\text{at} \qquad z = -h(x, y, t), \begin{cases} h_t + u_2 h_x + v_2 h_y = -w_2 & h > 0 \\ w_2 = 0 & h = 0 \end{cases} \text{ and } p_1 = p_2.$$

There is also a radiation condition that no energy must flow into the system from $|(y, z)| \to \infty$.

We now assume linear stratification, $\bar{\rho}_2 = \rho_0 + \bar{\rho}'_2 z$, $\bar{\rho}'_2 < 0$ a constant. $(\bar{\rho}_2(-h) - \rho_1)$ will vary with h but we will assume $|\bar{\rho}'_2 [h/(\rho_0 - \rho_1)]| \ll 1$ so that $\bar{\rho}_2(-h) - \rho_1 \simeq \rho_0 - \rho_1 = \Delta\rho$ a constant. In effect we are assuming that the basic density jump between the current and ocean layers is large compared to the density change within the ocean layer in the region of interest. This region will be seen to be near the surface. Let $P_{1,2} = p_{1,2} - g\Delta\rho h$ and nondimensionalize. We then have for the current:

$$\begin{aligned} u_{1t} + u_1 u_{1x} + v_1 u_{1y} - v_1 &= -h_x - P_{1x} \\ v_{1t} + u_1 v_{1x} + v_1 v_{1y} + u_1 &= -h_y - P_{1y} \\ h_t + (hv_1)_y + (hu_1)_x &= 0 \text{ (using the interface condition for the current)} \end{aligned} \tag{3}$$

for the ocean:

$$\begin{aligned} u_{2t} - v_2 &= -P_{2x} \\ v_{2t} + u_2 &= -P_{2y} \\ P_{2zt} + B^2 w_2 &= 0 \\ w_{2z} + v_{2y} + u_{2x} &= 0 \end{aligned} \tag{4}$$

and boundary conditions:

$$\text{at} \qquad z = -h(x, y, t), h_t + u_2 h_x + v_2 h_y = -w_2 \quad h > 0$$
$$0 = w_2 \quad h = 0$$
$$\text{and} \qquad P_1(x, y, t) = P_2(x, y, -h(x, y, t), t).$$

The nondimensionalizing was done as follows:

$h \sim H, z \sim H, x, y \sim L = \sqrt{g'H}/f$ (Rossby radius of deformation) $(u, v) \sim V_0 = \sqrt{g'H}, w \sim (H/L)\, V_0, t \sim 1/f, P \sim \rho_0 f L V_0$ (ρ_0/ρ_1, assumed $\simeq 1$) and $g' = g\,(\Delta\rho/\rho_0)$, $B = (H/L)(N/f)$ where buoyancy frequency $N = \sqrt{(-g/\rho_0)\,\bar{\rho}'_2}$ and B^2 is a Burger number.

Figure 1 shows the wedge-shaped front we are considering. For the steady state we

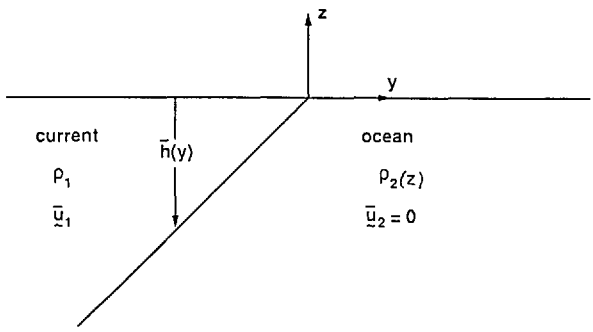

Figure 1. The canonical front (dimensionless space variables).

assume $\partial_x = \partial_t = 0, u_2 = v_2 = 0$ which implies $P_2 = 0$ so that $P_1 = 0$. For the current we assume $v_1 = 0$ and slope of the front is constant. Using overbars for steady state values we then have

$$\bar{u}_1 = -\bar{h}_y. \tag{5}$$

Thus for $\bar{h}_y$ constant $\bar{u}_1$ is constant, and assuming $\bar{u}_1$ is unity, $\bar{h}_y = -1$. Physically, there is no characteristic depth H, but rather the slope $m = H/L$ characterizes this flow. Dimensionally $\bar{h} = -my, \bar{u} = V_0$ so that given V_0 we have $m = fV_0/g', L = V_0/f$ and so $B = mN/f$. The dimensionless potential vorticity of the mean flow is $1/\bar{h}(y)$ which decreases away from the intersection of the front with the surface.

To be consistent with the assumption that $|\bar{\rho}'_2 [h/(\rho_0 - \rho_1)]| \ll 1$, we can show that we must have $B^2 \ll 1$. This is usually the case. For example for V_0 varying between 10 to 100 cm/sec, $N/f \simeq 100$ and $g' \simeq 3$ we have B varying from $\frac{1}{30}$ to $\frac{1}{3}$. However, this assumption could be violated for certain possible combinations of current speed, density gradient, and density jump between the layers.

The perturbation equations are found by expressing the dependent variables in steady and perturbation parts, i.e.

$( ) = (\bar{}) + ( )'$. Dropping the primes we find for the current:

$$\begin{aligned} u_{1t} + u_{1x} - v_1 &= -h_x - P_{1x} \\ v_{1t} + v_{1x} + u_1 &= -h_y - P_{1y} \\ h_t - (yv_1)_y - yu_{1x} + h_x &= 0 \end{aligned} \tag{6}$$

and for the ocean:

$$\begin{aligned} u_{2t} - v_2 &= -P_{2x} \\ v_{2t} + u_2 &= -P_{2y} \\ P_{2zt} + B^2 w_2 &= 0 \\ u_{2x} + v_{2y} + w_{2z} &= 0 \end{aligned} \tag{7}$$

with interface conditions:

$$\text{at} \qquad z = -\bar{h}(y), \begin{Bmatrix} h_t - v_2 = -w_2 & \bar{h} > 0 \\ 0 = w_2 & \bar{h} = 0 \end{Bmatrix} \text{ and } P_1 = P_2. \tag{8}$$

We do the usual linear stability analysis. We assume a plane wave solution in x:

$$(\ ) = (\hat{\ })e^{i(kx-\omega t)}. \tag{9}$$

For given values of the wavenumber k and the other parameters, we look for solutions of the eigenfrequency ω which have a positive imaginary part and are thus unstable.

Eliminating $\hat{u}_1$ and $\hat{v}_1$ in (6) we obtain for the current:

$$y\hat{h}_{yy} + \hat{h}_y + \left(\overline{D} - k^2 y - \frac{1}{1-c}\right)\hat{h} = -\left\{y\hat{P}_{yy} + \hat{P}_{1y} - \left(k^2 y + \frac{1}{1-c}\right)\hat{P}_1\right\} \tag{10}$$

where $c = \omega/k$ and $\overline{D} = 1 - k^2(1-c)^2$. Boundary conditions associated with (10) are that (6c) be satisfied at $y = 0$ (which will imply that $\hat{h}$ be bounded at $y = 0$) and that $\hat{h}$ be bounded for $y \to -\infty$.

For the ocean, eliminating $\hat{u}_2, \hat{v}_2, \hat{w}_2$ in (7) we obtain:

$$\nu^2\hat{P}_{2zz} - \hat{P}_{2yy} + k^2\hat{P}_2 = 0 \tag{11}$$

where $\nu^2 = (\omega^2 - 1)/B^2$. Though we are assuming $B^2 \ll 1$, ν^2 cannot be assumed to be always large since $\omega^2 - 1$ can be small. The boundary conditions associated with this equation are:

$$\begin{aligned} &\text{at} \qquad z = y, y < 0\text{: } -i\omega\hat{h} - \hat{v}_2 = -\hat{w}_2 \text{ or } B^2\nu^2\hat{h} = \hat{P}_{2y} + \frac{k}{\omega}\hat{P}_2 + \nu^2\hat{P}_{2z} \\ &\text{at} \qquad z = 0, y > 0\text{: } \hat{w}_2 = 0 \end{aligned} \tag{12}$$

and the radiation condition for $|y, z| \to \infty$.

3. Energy balance

Before finding a solution to the system of equations, it will be useful to have the perturbation energy flux balance in the current layer. This can be shown to be in dimensionless form:

$$\frac{\partial}{\partial t}\left\{\overline{\bar{h}\frac{1}{2}(u^2 + v^2)} + \overline{\frac{1}{2}h^2}\right\} = -\overline{\bar{u}_1\bar{h}_x P_1} + \overline{(w_2 + \bar{h}_y v_2)P_1} - \frac{\partial}{\partial y}\left[\overline{\bar{h}\,v_1(P_1 + h)}\right] \tag{13}$$

where we have integrated over the depth of the current layer and the long overbar is an average over x ($\bar{h}$ and $\bar{u}_1$ are still the steady state quantities). The terms on the left

are the rate of change of the kinetic energy density and the potential energy density. The first term on the right is the energy flux from the mean flow, the second term the energy flux out of the current layer (internal wave radiation) and the third term the lateral flux within the layer.

It will be useful to see how well our asymptotic solutions satisfy this equation. We will integrate it over y from 0 to $-\infty$ in which case the third term on the right will vanish.

4. Solution for special case: no stratification

For no stratification in the ocean, $B = 0$ which means $P_2 = P_1 = 0$. From (10) we then have

$$Y\hat{h}_{YY} + \hat{h}_Y + (K - \tfrac{1}{4}Y)\,\hat{h} = 0 \tag{14}$$

where $Y = -2\,|k|\,y$ and $K = [c/(1-c) + k^2\,(1-c)^2]/2\,|k|$. The boundary conditions are: at $Y = 0$, $\hat{h}_Y = -K\hat{h}$ and for $Y \to \infty$, $\hat{h}$ bounded. A solution of (14) which is bounded at $Y = 0$ automatically satisfies the boundary condition at $Y = 0$. The general solution is

$$\hat{h} = e^{-Y/2}[C_1 M(\tfrac{1}{2} - K, 1, Y) + C_2 U(\tfrac{1}{2} - K, 1, Y)] \tag{15}$$

where M and U are confluent hypergeometric functions. The property of these functions is such that $\hat{h}$ will be unbounded at $Y = 0$ or $Y \to \infty$ unless $1/\Gamma(\tfrac{1}{2} - K) = 0$. So our eigenvalues are given by the equation

$$K = n + \tfrac{1}{2},\ n = 0, 1, 2, \ldots \tag{16}$$

For these values we can show that eigenfunctions are

$$\hat{h}_n = C_n e^{-Y/2} L_n(Y) \tag{17}$$

where the Laguerre polynomial, $L_n(Y) = \Sigma_{j=0}^{n}(-1)^j \binom{n}{j} (1/j!)\, Y^j$. Thus, we obtain finite degree polynomials consistent with the work of Cushman-Roisin (1986b) and Ripa (1987).

From (16) we have the cubic equation:

$$(c-1)^3 - \left[\frac{2n+1}{|k|} + \frac{1}{k^2}\right](c-1) - \frac{1}{k^2} = 0. \tag{18}$$

The discriminant is $(1/4k^4) - (1/27)[(2n+1)/|k| + (1/k^2)]^3$ which is $(1/-27k^4) \times (|k| - 2)^2\,[|k| + (1/4)] \leq 0$ for $n = 0$. If the discriminant is ≤ 0 for $n = 0$ then it also is for $n > 0$, so it is ≤ 0 for all $n \geq 0$, and there are only real roots for $\omega = ck$. Thus the nonstratified case is always neutrally stable.

Interestingly, Orlanski (1968) analyzed a flow with similar geometry but with a bottom boundary and found the flow to be unstable. We note that we do not have the long wave, low frequency instability of quasi-geostrophic theory (baroclinic instability). The results most resemble that of Paldor (1983).

5. Asymptotic solution for stratified ocean ($B > 0$)

a. Rays in the ocean. We assume $|k| \gg 1$ and in the ocean let

$$\hat{P} = A(y, z)e^{i|k|S(y,z)} \tag{19}$$

and use ray theory (Kroll, 1975). Eq. 11 becomes

$$\nu^2\left[\frac{1}{k^2}A_{zz} + \frac{2i}{|k|}S_zA_z + \frac{i}{|k|}S_{zz}A - S_z^2A\right] - \left[\frac{1}{k^2}A_{yy} + \frac{2i}{|k|}S_yA_y + \frac{i}{|k|}S_{yy}A - S_y^2A\right] + A = 0 \tag{20}$$

where we assume $A = A_0 + (1/|k|)A_1 + \ldots$.

We assume $\nu = 0(1)$. If ν is large then one should define a new vertical variable $\bar{z} = z/|\nu|$ for proper ordering in $1/k$. However, in assuming $\nu = 0(1)$, we retain the same terms at each order as when $\bar{z}$ is used. To lowest order in $1/|k|$ we obtain the eiconal equation:

$$F(y, z, p, q, S) = -\nu^2q^2 + p^2 + 1 = 0 \tag{21}$$

where $p = S_y$ and $q = S_z$ are wavenumbers in y and z respectively. To solve this equation we use characteristics derived from the parametric differential equations:

$$\frac{dy}{ds} = F_p, \frac{dz}{ds} = F_q, \frac{dp}{ds} = -F_y, \frac{dq}{ds} = -F_z, \frac{dS}{ds} = pF_p + qF_q. \tag{22}$$

On the interface $z = y$ we define $s = 0$ and $z = y = \tau$. The parameters s and τ are the ray variables. (Actually the derivatives in (22) should be written as partial derivatives but traditionally are not.)

From (22) we find the wavenumbers are constant on any given ray: $p = \bar{p}(\tau)$ and $q = \bar{q}(\tau)$. The rays are given by the parametric equations:

$$y = 2\bar{p}s + \tau, z = -2\nu^2\bar{q}s + \tau. \tag{23}$$

In addition we have the strip condition at $s = 0$: $dS/d\tau = p\ (dy/d\tau) + q\ (dz/d\tau)$, which implies that

$$\bar{S}'(\tau) \equiv \frac{d\bar{S}}{d\tau} = \bar{p}(\tau) + \bar{q}(\tau) \tag{24}$$

where $\bar{S}(\tau)$ will be S given at the interface. Combining (21) and (24) we find:

$$\bar{p} = \frac{-\nu^2\bar{S}' + \sqrt{\nu^2\bar{S}'^2 + \nu^2 - 1}}{1 - \nu^2} \quad \text{and} \quad \bar{q} = \frac{\bar{S}' - \sqrt{\nu^2\bar{S}'^2 + \nu^2 - 1}}{1 - \nu^2}. \tag{25}$$

Also we can find $S(s, \tau)$ using the last equation of (22):

$$S(s, \tau) = -2s + \bar{S}(\tau) \tag{26}$$

The proper sign for the radical in (25) was determined by the radiation condition. The coordinate normal to the interface and positive downward is $\eta = y - z$. The group speed $d\eta/dt$ must then be positive (radiation condition). If the time, t, is not removed from the original system we can show that $dt/ds = -F_\omega = 2q^2\omega/B^2$ so that

$$\frac{d\eta}{dt} = \frac{d}{ds}(y - z)\frac{ds}{dt} = \frac{B^2}{q^2\omega}(\bar{p} + \nu^2\bar{q}) = \frac{B^2}{q^2\omega}\sqrt{\nu^2\bar{S}'^2 + \nu^2 - 1}\,. \tag{27}$$

(This can also be found using the second term on the right of (13), the energy flux evaluated at the interface.) So the sign was chosen so that $d\eta/dt > 0$ for $d\eta/dt$ real when ω is real and positive.

From (22) the slope of the rays is given by:

$$\frac{dz}{dy} = \frac{1 + \bar{S}'\nu\sqrt{\bar{S}'^2 - (1 - \nu^2)/\nu^2}}{1/\nu^2 - \bar{S}'^2}. \tag{28}$$

We have two sets of rays according to $\bar{S}'(\tau) \gtrless 0$. On Figure 2 we illustrate a ray pair from one point on the interface for various conditions.

From the next higher order in $1/|k|$ in (20) we obtain an equation for the amplitude to lowest order:

$$2[\nu^2 S_z A_{0z} - S_y A_{0y}] + (\nu^2 S_{zz} - S_{yy})A_0 = 0 \tag{29}$$

We note that $dA/ds = A_z\,(dz/ds) + A_y\,(dy/ds) = -2\nu^2 qA_z + 2pA_y$. Hence

$$\frac{dA_0}{ds} - (\nu^2 S_{zz} - S_{yy})A_0 = 0. \tag{30}$$

To evaluate S_{zz} and S_{yy} we note that $S_{zz} = \bar{q}_z = \bar{q}_\tau\,(\partial\tau/\partial z)$ and $S_{yy} = \bar{p}_y = \bar{p}_\tau\,(\partial\tau/\partial y)$ and find $\partial\tau/\partial y$ and $\partial\tau/\partial z$ from implicit differentiation of the ray equations of (23). We can then show that

$$\frac{dA_0}{ds} + \frac{\nu^2\alpha}{2\nu^2\alpha s - D_0}A_0 = 0 \tag{31}$$

where $\alpha = \bar{p}\bar{q}_\tau - \bar{q}\bar{p}_\tau = -(\bar{S}''/D_0)$ and $D_0 = \sqrt{\nu^2\bar{S}'^2 + \nu^2 - 1}$.

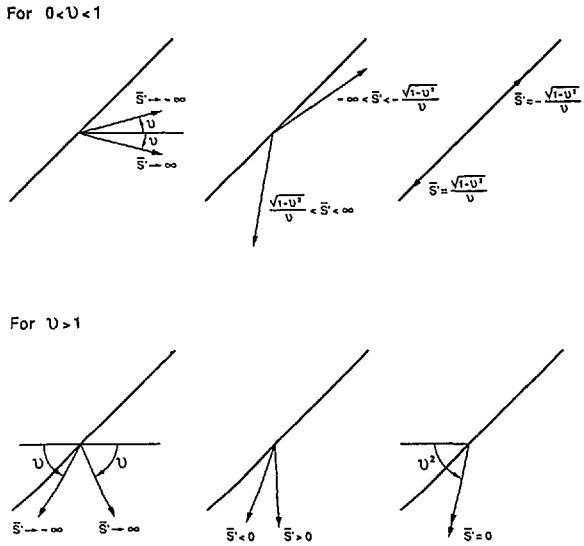

Figure 2. Ray pair from one point on the interface for various values of $\bar{S}'$ and ν. The angle measures represent slope.

The solution can be written as

$$A_0(s, \tau) = G(\tau)(D_0^2 + 2\nu^2\bar{S}''s)^{-1/2} \tag{32}$$

where $G(\tau)$ is an arbitrary function of τ.

b. Asymptotic solution in the current for $|k| \gg 1$. For the current let $\hat{h} = (-2|k|y)^{-1/2} H(y)$ and $\hat{P}_1 = (-2|k|Y)^{-1/2}R(y)$ in (10):

$$H'' - \left\{\frac{k^2(y + \bar{y}_c)}{y} - \frac{1/4}{y^2}\right\} H = -\left\{R'' - \left[k^2 + \frac{1}{(1-c)y} - \frac{1/4}{y^2}\right]R\right\} \tag{33}$$

where $\bar{y}_c = (2|k|K/k^2) = (1/k^2)[c/(1-c) + k^2(1-c)^2]$. For k^2 large, $y = -\bar{y}_c$ is a turning point of the left side of (33). For $-\bar{y}_c < y < 0$ but y not near $-\bar{y}_c$ or 0 we look for an oscillatory solution. So we assume

$$\hat{h} = \mathscr{A}e^{i|k|\bar{S}(y)} \tag{34}$$

where $\mathscr{A} = \mathscr{A}_0 + (1/|k|)\mathscr{A}_1 + \ldots$.

For $\hat{P}_2 = A_0 e^{i|k|S(y,z)}$, the interface condition (12) then yields to lowest order

$$A_0(0, \tau) = \frac{\nu^2 B \mathscr{A}_0}{i|k|\left(D_0 - \dfrac{ik}{\omega|k|}\right)} \tag{35}$$

where at $s = 0$, $S(y,z) = S(y,y) = \bar{S}(y) = \bar{S}(\tau)$. From (32) for $s = 0$, we then have $G(\tau) = \nu^2 B^2 \mathscr{H}_0(\tau)/\, i|k|[1 - (ifk/\omega D_0|k|)]$, so

$$A_0(s,\tau) = \frac{\nu^2 B^2 \mathscr{H}_0(\tau)}{i|k|\left[1 - \dfrac{ik}{\omega D_0|k|}\right]\sqrt{D_0^2 + 2\nu^2 \bar{S}'' s}}. \tag{36}$$

The radical in the denominator can vanish for $\bar{S}' < 0$ which will be a caustic of the wave field.

Similarly to (34) for $-\bar{y}_c < y < 0$, we let $H = \mathscr{H} e^{i|k|\bar{S}(y)}$ and, using the fact that $\hat{P}$ is continuous at $z = y$ and that $A_0 = 0[(1/|k|)]\hat{h}_0$, we let $R = (\mathscr{R}/|k|)e^{i|k|\bar{S}(y)}$. Then (33) becomes:

$$\frac{1}{k^2}\mathscr{H}'' + \frac{2i}{|k|}\bar{S}'\mathscr{H}' + \frac{i}{|k|}\bar{S}''\mathscr{H} - \bar{S}'^2\mathscr{H} - \left\{\frac{y + \bar{y}_c}{y} - \frac{1/4}{k^2 y^2}\right\}\mathscr{H}$$
$$= -\left\{\frac{1}{|k|^3}\mathscr{R}'' + \frac{2i\bar{S}'}{k^2}\mathscr{R}' + \frac{i\bar{S}''}{k^2}\mathscr{R} - \frac{\bar{S}'^2}{|k|}\mathscr{R} - \left(\frac{1}{|k|} + \frac{1}{|k|^3(1-c)y} - \frac{1/4}{|k|^3 y^2}\right)\mathscr{R}\right\} \tag{37}$$

where $\mathscr{H} = \mathscr{H}_0 + (1/|k|)\mathscr{H}_1 + \ldots, \mathscr{R} = \mathscr{R}_0 + (1/|k|)\mathscr{R}_1 + \ldots$.

For the lowest order we have

$$\bar{S}'(y) = \pm\bar{\sigma}'(y) \tag{38}$$

where

$$\bar{\sigma}'(y) = \sqrt{\frac{y+\bar{y}_c}{-y}},\ y < 0.$$

For the next order we have

$$2i\bar{S}'\mathscr{H}'_0 + i\bar{S}''\mathscr{H}_0 = (\bar{S}'^2 + 1)\mathscr{R}_0 \tag{39}$$

c. Connecting rays with the current. $\mathscr{H}_0$ and $\mathscr{R}_0$ are connected at $s = 0$ using (35):

$$\mathscr{R}_0 = (-2|k|y)^{1/2}|k|A_0 = \frac{-i(\omega^2 - 1)}{\left(D_0 - \dfrac{ik}{\omega|k|}\right)}\mathscr{H}_0$$

So we have

$$\mathscr{H}'_0 + \left[\frac{1}{2}\frac{\bar{S}''}{\bar{S}'} + \frac{(\omega^2 - 1)}{2\bar{S}'}\frac{(\bar{S}'^2 + 1)}{D_0 - \dfrac{ik}{\omega|k|}}\right]\mathscr{H}_0 = 0 \tag{40}$$

which has a solution in the form

$$\mathscr{H}_0 = \frac{C}{\sqrt{\bar{S}'}} e^{-(\omega^2-1)snI(-y)/2} \tag{41}$$

where *sn* is the sign in (38) and

$$I(-y) = \int_0^y \frac{\bar{y}_c/-y'}{\sqrt{\dfrac{y'+\bar{y}_c}{-y'}}\left[\sqrt{\dfrac{\nu^2\bar{y}_c+y'}{-y'}} - \dfrac{ik}{\omega|k|}\right]} dy', \tag{42}$$

using the fact that

$$D_0 = \sqrt{\nu^2\bar{S}'^2 + \nu - 1} = \sqrt{\frac{\nu^2\bar{y}_c + y}{-y}}.$$

The integral (42) can be integrated in terms of elementary functions. Its form will depend on whether or not $\nu^2 > 1$, and the behavior of D_0 when $y < \nu^2\bar{y}_c$. In the ocean, $e^{i|k|S(y,z)} = e^{i|k|(-2s+\bar{S}(\tau))}$ from (26). This term must decay moving away from the interface when $y < \nu^2\bar{y}_c$. We can show that $s = (y-z)/2D_0$ and $y - z$ increases away from the interface. Therefore if $y = z < -\nu^2\bar{y}_c$ then $D_0 = i\sqrt{-(y+\nu^2\bar{y}_c)/-y}$ so that $e^{-2i|k|s}$ decays. This also means that the pole from the bracketed term in (42) can occur only for $y < -\nu^2\bar{y}_c$ and $k > 0$ for $\omega > 0$.

To integrate (42) we let $y = -\bar{y}$ so $\bar{y} > 0$, and we can show that

$$I(\bar{y}) = -\frac{\bar{y}_c\omega^2}{\omega^2-1}\left\{\int_0^{\bar{y}} \frac{\sqrt{\nu^2\bar{y}_c - \bar{y}'}}{\sqrt{\bar{y}_c - \bar{y}'}(\bar{y}_p - \bar{y}')} d\bar{y}' + \frac{ik}{\omega|k|}\int_0^{\bar{y}} \frac{\sqrt{y'}}{\sqrt{\bar{y}_c - \bar{y}'}(\bar{y}_p - \bar{y}')} d\bar{y}'\right\} \tag{43}$$

where $\bar{y}_p = (\omega^2/B^2)\bar{y}_c$. If we let $\mu^2 = (\nu^2\bar{y}_c - \bar{y})/(\bar{y}_c - \bar{y})$, the first integral can be evaluated and letting $\bar{\mu}^2 = \bar{y}/(\bar{y}_c - \bar{y})$ the second can be evaluated. The result, valid for $0 < \bar{y} < \bar{y}_c < \nu^2\bar{y}_c < \bar{y}_p$ (consistent with $\nu^2 > 1$, $\omega^2 > B^2$) is

$$I(\bar{y}) = \frac{-\bar{y}_c\omega^2}{\omega^2-1}\left\{\operatorname{Log}\frac{(\mu-1)(\nu+1)}{(\mu+1)(\nu-1)} - \mu_0 \operatorname{Log}\frac{(\mu-\mu_0)(\nu+\mu_0)}{(\mu+\mu_0)(\nu-\mu_0)} - \frac{2ik}{\omega|k|}\left(\tan^{-1}\bar{\mu} - \bar{\mu}_0\tan^{-1}\frac{\bar{\mu}}{\bar{\mu}_0}\right)\right\} \tag{44}$$

where $\mu_0^2 = (\bar{y}_p - \nu^2\bar{y}_c)/(\bar{y}_p - \bar{y}_c) = 1/(\omega^2 - B^2)$ and $\bar{\mu}_0^2 = \bar{y}_p/(\bar{y}_p - \bar{y}_c) = \omega^2/(\omega^2 - B^2)$. We are interested essentially in $0 < \bar{y} < \bar{y}_c$ but also need solutions for $\nu^2 < 1$ and $\omega^2 < B^2$. Moreover, $\bar{y}_c$, $\nu^2\bar{y}_c$ and $\bar{y}_p$ can be complex for ω complex. We can show that (44) is consistent with the required decay property of D_0 in (42) for all cases for our parameters including complex values when the cut for the log and $\tan^{-1}$ function is taken down the negative imaginary axis and the same cut for $\sqrt{\omega^2-1}$ and $\sqrt{\omega^2 - B^2}$.

The result above also includes the case for $\bar{y}_p < \bar{y}_c$ ($\omega^2 < B^2$) when a log singularity occurs for $\bar{y} = \bar{y}_p$. To properly deal with it, one goes back to the original system and looks for a boundary layer about $\bar{y} = \bar{y}_p$ which turns out to be $0(1/\sqrt{|k|})$. Using (32) in (18), the interface condition (12) becomes

$$B^2\nu^2\hat{h} = \frac{e^{i|k|S}}{D_0}\left\{kG(y)\left[i(\bar{p} + \nu^2\bar{q}) + \frac{1}{\omega}\right] + G'(y)\frac{\nu^2}{D_0}(\bar{q} + \bar{p})\right\} \tag{45}$$

Using $\hat{h}$ from above, $\hat{P} = G(y)e^{i|k|\bar{S}(y)}/D_0$ for $s = 0$, and letting $y = -\bar{y}_p - \eta/\sqrt{|k|}$ in (33), we find to lowest order in $1/\sqrt{|k|}$ that $\bar{S}'^2 = \bar{S}'^2_0 = (\bar{y}_c - \bar{y}_p)/\bar{y}_p$ which implies that $i(\bar{p} + \nu^2\bar{q}) + 1/\omega = i\sqrt{\nu^2\bar{S}'^2 + \nu_2 - 1} + 1/\omega = 0$. The next order then yields

$$G_{\eta\eta} - i\beta\eta G_\eta + bG = 0 \tag{46}$$

where $\beta = \bar{y}_c/2\bar{S}'_0\bar{y}_p^2$ and $b = B^2\bar{y}_c/2\omega\bar{S}'^2_0\bar{y}_p$. We can show that the solution which for $\eta \to \pm\infty$ matches (41) is

$$G(\eta) = C_0 e^{i\beta\eta^2/4}E^*(a, \sqrt{\beta}\eta) \tag{47}$$

where E^* is the complex form of a parabolic cylindrical function and $a = -[(b/\beta) + (i/2)]$. $E^*(a, 0)$ is finite so there is actually no singularity. We can show that $G(\eta \to -\infty) = ie^{\pi a}G(\eta \to \infty)$ and show that this property is preserved by (44). To lowest order we will neglect the correction due to this boundary layer and also neglect correcting for the even more singular case when $\omega = B$ ($\bar{y}_p = \bar{y}_c$). We will use (44) for all cases.

So putting it all together for both signs, we have

$$\hat{h}_0 = \frac{1}{\sqrt{-2|k|y}}\left\{\frac{C_1}{\sqrt{\bar{\sigma}'}}e^{-[(\omega^2-1)/2]I}e^{i|k|\bar{\sigma}} + \frac{C_2}{\sqrt{\bar{\sigma}'}}e^{[(\omega^2-1)/2]I}e^{-i|k|\bar{\sigma}}\right\} \tag{48}$$

d. Expansions about special points. So far we have a lowest order solution in the current for $0 < y < -\bar{y}_c$ away from the turning point $y = -\bar{y}_c$ and the singular point and boundary point $y = 0$.

We can show from (33) there is a boundary layer of $0(1/k^2)$ near $y = 0$. We let $y = -\xi/k^2$ and can show that $R = 0(1/k^2)$ H from (12), using the ray solution. So to lowest order (33) becomes

$$H_{0\xi\xi} + \left[\frac{\bar{y}_c}{\xi} + \frac{1/4}{\xi^2}\right]H_0 = 0 \tag{49}$$

The solution which yields bounded $\hat{h}_0$ is

$$H_0 = D'_1\sqrt{\xi}J_0(2\sqrt{\bar{y}_c\xi}) \qquad \text{or} \qquad \hat{h}_0 = D_1J_0(2\sqrt{\bar{y}_c\xi}) \tag{50}$$

This solution must match (48). From (38)

$$\bar{\sigma}(y) = \int_0^y \sqrt{\frac{y' + \bar{y}_c}{-y'}}\, dy' = y\sqrt{\frac{y + \bar{y}_c}{-y}} + \bar{y}_c\left[\tan^{-1}\sqrt{\frac{y + \bar{y}_c}{-y}} - \frac{\pi}{2}\right] \tag{51}$$

Noting that for $y \to 0$, $\bar{\sigma}' \to \sqrt{\bar{y}_c}\,|k|/\sqrt{\xi}$, $\bar{\sigma} \to (-2\sqrt{\bar{y}_c}/|k|)\sqrt{\xi}$ and $I \to 0$ in (48) and using the asymptotic expansion of $J_0(2\sqrt{\bar{y}_c\xi})$ for ξ large, we find the common part to be

$$\hat{h}_0 = \frac{D_1}{\sqrt{\pi}\,(\bar{y}_c\xi)^{1/4}}\left[e^{i[2\sqrt{\bar{y}_c\xi} - (\pi/4)]} + e^{-i[2\sqrt{\bar{y}_c\xi} - (\pi/4)]}\right] \tag{52}$$

and

$$C_1 = \frac{D_1 e^{i(\pi/4)}}{\sqrt{2\pi}}, \qquad C_2 = \frac{D_1 e^{-i(\pi/4)}}{\sqrt{2\pi}}$$

For $y \to \bar{y}_c$ we can show from (33) that there is an $0(|k|)^{-2/3})$ boundary layer about the turning point $y = -\bar{y}_c$. We let $y + \bar{y}_c = \zeta/|k|^{2/3}$ and can show $R = 0(1/|k|)H$. So to lowest order (33) becomes

$$H_{0\zeta\zeta} + \frac{\zeta}{\bar{y}_c} H_0 = 0 \tag{53}$$

having the solution

$$H_0 = B_0 Ai\left(\frac{-\zeta}{\bar{y}_c^{1/3}}\right) \qquad \text{or} \qquad \hat{h}_0 = \frac{B_0}{\sqrt{-2|k|y}} Ai\left(\frac{-\zeta}{\bar{y}_c^{1/3}}\right). \tag{54}$$

We match this for $\zeta \to \infty$ to (48) for $y \to -\bar{y}_c$. Using the asymptotic expansion of the Airy function, $Ai(z)$, we have the common part

$$\hat{h}_0 = \frac{B_0 \bar{y}_c^{1/12}}{2i\zeta^{1/4}\sqrt{2\pi|k|\bar{y}_c}}\left\{e^{i(\pi/4)}e^{2/3(\bar{y}_c^{-1/2}\zeta^{3/2})} - e^{-i(\pi/4)}e^{-2/3(\bar{y}_c^{-1/2}\zeta^{3/2})}\right\}. \tag{55}$$

We note that for $y \to -\bar{y}_c$, $\bar{\sigma}' \to |k|^{-1/3}\,\bar{y}_c^{-1/2}\,\zeta^{1/2}$ and $\bar{\sigma} \to \frac{2}{3}|k|^{-1}\,\bar{y}_c^{-1/2}\,\zeta^{3/2} - (\pi/2)\,\bar{y}_c$ and match (55) with (48) and obtain

$$C_1|k|^{1/6}\bar{y}_c^{1/4}e^{-(\omega^2-1)I(\bar{y}_c)/2}e^{-i(\pi/2)|k|\bar{y}_c} = \frac{B_0\bar{y}_c^{1/12}}{2i\sqrt{\pi}}e^{i(\pi/4)} \qquad \text{and}$$

$$C_2|k|^{1/6}\bar{y}_c^{1/4}e^{(\omega^2-1)I(\bar{y}_c)/2}e^{i(\pi/2)|k|\bar{y}_c} = \frac{-B_0\bar{y}_c^{1/12}}{2i\sqrt{\pi}}e^{-i(\pi/4)}$$

where $I(\bar{y}_c)$ is $I(-y)$ evaluated at $\bar{y} = -y = \bar{y}_c$ from (44). Eliminating C_1 and C_2 using

(52) we can show that the eigenvalues are given by

$$\cos\left\{\frac{|k|\pi}{2}\bar{y}_c - \frac{i(\omega^2-1)}{2}I(\bar{y}_c)\right\} = 0$$
$$\text{or} \quad \frac{|k|\pi}{2}\bar{y}_c - \frac{i(\omega^2-1)}{2}I(\bar{y}_c) = \frac{\pi}{2}(2n+1) \tag{56}$$

$n = 0, 1, 2, \ldots$. Based on the exact solution for no stratification, (16), we assume $n \geq 0$ only. Rewriting (56) we have

$$\bar{y}_c\left\{1 + \frac{i\omega^2}{\pi|k|}M(\omega)\right\} = \frac{2n+1}{|k|} \tag{57}$$

where $M(\omega) = \text{Log}\,[(\nu+1)/(\nu-1)] - \mu_0\,\text{Log}\,[(\nu+\mu_0)/(\nu-\mu_0)] - i\pi k(1-\bar{\mu}_0)/|k|\omega$ with μ_0 and $\bar{\mu}_0$ defined in (44) and cuts for complex functions as described for (44).

We would like to calculate the solution for higher order terms, but this was not done because the equations become excessively more complicated. However, let us look at our scaling after the fact. For $(2n+1)/|k| \ll 1$, the unstable solution can be shown to have $\omega \sim k$ implying $\nu \gg 1$ so that (35) implies that $P = 0(B)h$. So in actuality we must also have $B \ll 1$ for asymptotic validity. But this is consistent with our assumptions for the model. For $\nu = 0(1)$, (35) implies that $P = 0(B^2/|k|)\,h$.

An analysis of the next order for the ray solution in the ocean away from any caustics yields $(1/|k|)\,A_1/A_0 \simeq (3/8)/(2n+1)$ for $\nu \geq 0(1)$ and $\simeq 0(\nu^4)$ for $\nu \ll 1$. Clearly we should expect the best quantitative accuracy for $B \ll 1$ and n large. However, the similarity of the stability patterns for all n suggest that even the $n = 0$ case is at least qualitatively useful. Since the model itself is only an approximation of a portion of a real flow, qualitative results are most important. Results using our solution in the energy balance will be discussed later but are encouraging.

Let us examine (57). For $B = 0$ then $M = 0$ so we have $\bar{y}_c = 2K/|k| = (2n+1)/|k|$ which is the exact solution previously found from (16). Thus our asymptotic solution for the eigenvalues for this special case is exact. The asymptotic eigenfunctions are certainly not exact. This degree of agreement does not mean we can expect similar accuracy for the $B > 0$ case, but it is not discouraging.

We saw from (18) that the eigenvalues for the $B = 0$ case are always real. For $0 < B \ll 1$, $|k|$ large and $Re(\omega) > 1$ we can show that (57) can be written approximately

$$\bar{y}_c\left\{1 + \frac{i}{|k|}\left[\frac{2B}{\pi}\sqrt{\omega^2-1} + \frac{iB^2}{2\omega}\right]\right\} = \frac{2n+1}{|k|} \tag{58}$$

where $\bar{y}_c = (1-c)^2 + (1/k^2)\,(c/(1-c))$. For $|k|$ large and $B = 0$, we have to lowest order the three roots $1 - c = \pm\sqrt{(2n+1)/|k|}$ and $1 - c = 1/|k|(2n+1)$. Assuming

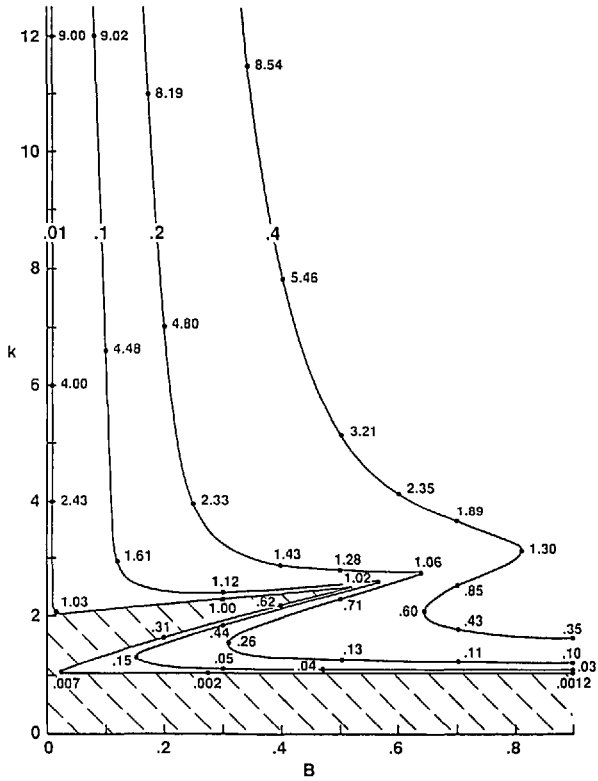

Figure 3. The unstable root: $n = 0$. Contours of constant values of the imaginary part of eigenfrequency (ω_i). Smaller numbers along contours are the real part of eigenfrequency (ω_r). Shaded regions are neutral.

$B \leq 0(1/\sqrt{|k|})$ we can show from (58) that

$$\omega \simeq k\left[1 \mp \sqrt{\frac{2n+1}{|k|}} \pm \frac{iB}{\pi}\sqrt{\frac{2n+1}{|k|}}\left(1 \mp \sqrt{\frac{2n+1}{|k|}}\right) + \cdots\right] \tag{59}$$

for two of the roots and for the other

$$\omega \simeq k\left[1 - \frac{1}{|k|(2n+1)} - \frac{2iB}{\pi k(2n+1)} + \cdots\right]. \tag{60}$$

Only the root for the top sign in (59) can be unstable ($Im(\omega) > 0$). This is for $k > 0$ and $1 > \sqrt{(2n+1/|k|)}$. If $k < 0$ and $1 > \sqrt{(2n+1)/|k|}$ then $Re(\omega) < 0$ and these results are invalid since we assumed $Re(\omega) > 0$ in our radiation condition. If proper adjustments are made, the $Re(\omega) < 0$ case can be resolved and it can be shown that the only unstable case is the one mentioned above. For $1 < \sqrt{(2n+1)/|k|}$, (59) is not valid, but the numerical solution of (57) shows there are no unstable waves in this case. Thus one of the three roots for the $B = 0$ case becomes unstable immediately

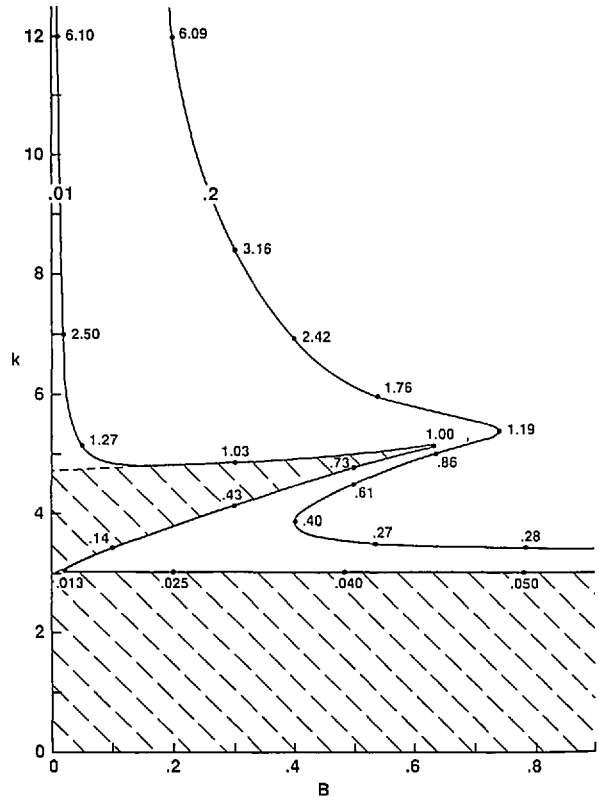

Figure 4. The unstable root: $n = 1$.

for increasing B if $(2n + 1)/|k| < 1$. This unstable wave is in the direction of the current.

6. Results and discussion

Figures 3, 4, and 5 show the solution of (57) for $n = 0$, 1 and 5 of the one unstable root. The contours are of constant $Im(\omega) = \omega_i$, the shaded regions are neutrally stable, and the numbers along the curves are values of $Re(\omega) = \omega_r$. In every case there is no instability for $k < 2n + 1$. The graphs tend to be divided in two regions: A subinertial region ($Re(\omega) < 1$) with a wedge shape for k in the neighborhood of $2n + 1$ and a superinertial region ($Re(\omega) > 1$) for larger k. In general we have a greater instability for increasing k and increasing B.

The pattern of Figures 3, 4 and 5 remains similar as n is increased but the pattern is translated by $k = 2n$. Figure 6 shows how at a point $B = .4$, $k = 5 + 2n$ the field changes little for increasing n for $n \geq 5$. Thus the form of the field is fairly constant for n for the proper translation in k.

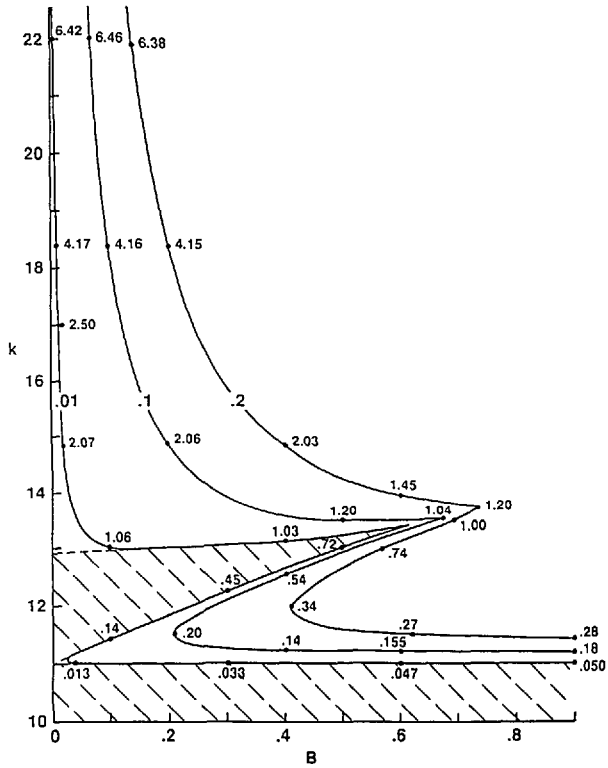

Figure 5. The unstable root: $n = 5$.

Let us consider the flow of energy away from the interface associated with the instability. The portion of the interface from which we can have wave propagation is controlled by two overlapping "windows": $-\bar{y}_c < y < 0$ and $-\nu^2 \bar{y}_c < y < 0$. The "current window" is determined by the current layer where the portion of the interface for $y < -\bar{y}_c$ will have an exponentially decaying field in the current with $\overline{S}'^2 < 0$ yielding complex values for $\bar{p}$ and $\bar{q}$ and thus an exponentially decaying field in the ocean. The "ocean window" is determined by an interaction of the current and the ocean where the portion of the interface for $y < -\nu^2 \bar{y}_c$ will yield complex values for $\bar{p}$ and $\bar{q}$ and exponential decay also. Thus the least open window determines the extent of the propagation from the interface. For $\nu^2 > 1$ the interval is $[-\bar{y}_c, 0]$ and for $\nu^2 < 1$ it is $[-\nu^2 \bar{y}_c, 0]$.

For B fixed and k increasing, $\bar{y}_c$ decreases and ν^2 becomes > 1 and increases. So for increasingly large k, $\bar{y}_c \to 0$ and the window is closing down even though ω_i is increasing. An analysis of the energy flux through the window reveals that it remains approximately constant as $\bar{y}_c \to 0$ (the flux density increases) for a fixed average value for the initial perturbation of h. So we get an increasingly more concentrated beam as k increases. On the other hand for decreasing k, ν^2 becomes < 1 and decreases so

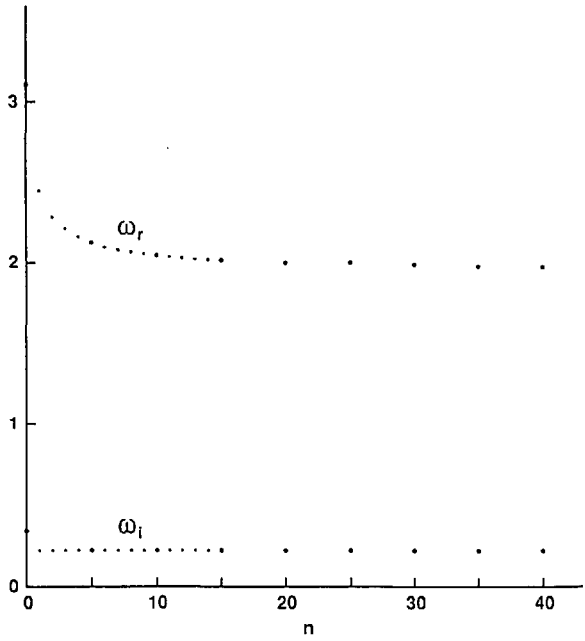

Figure 6. Typical variation of unstable eigenfrequency, ω with n for $B = .4$ and $k = 5 + 2n$.

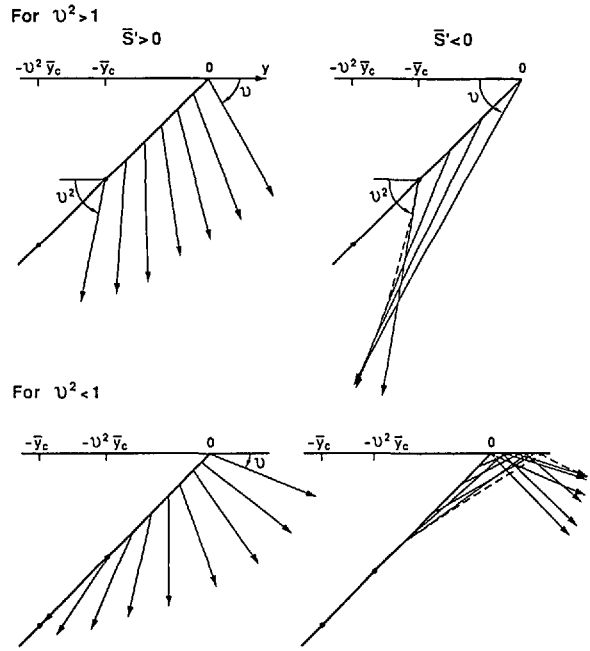

Figure 7. Typical ray fields in dimensionless space for $\bar{S}' \gtrless 0$ and $\nu^2 \gtrless 1$. Dashed lines are envelopes of rays, caustics in the field. The angle measures represent slope.

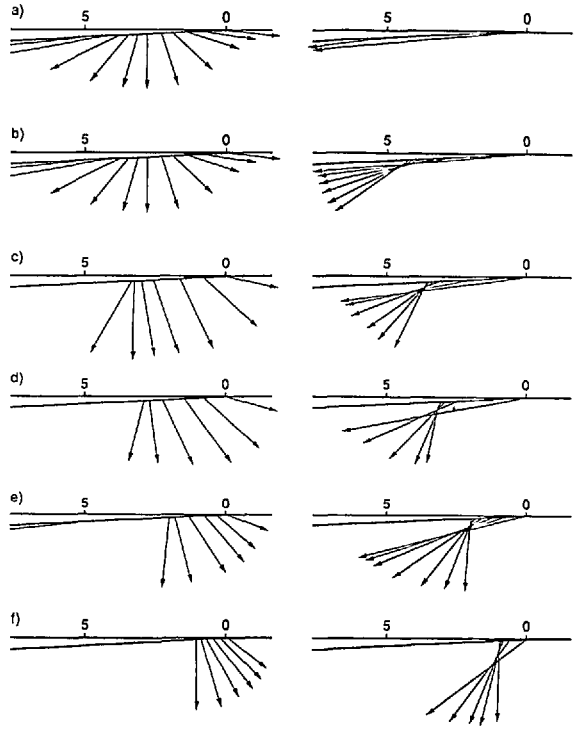

Figure 8. Typical ray fields in dimensional space as k increases. The horizontal scale is in kilometers. The left column is for $\overline{S}' > 0$, the right $\overline{S}' < 0$. The conditions (dimensionless) are: (a) $k = 2.1$, $\omega = 1.001 + .025i$; (b) $k = 2.5$, $\omega = 1.30 + .078i$; (c) $k = 3.0$, $\omega = 1.67 + .088i$; (d) $k = 3.5$, $\omega = 2.05 + .090i$; (e) $k = 5$, $\omega = 3.20 + .094i$; (f) $k = 10$, $\omega = 7.30 + .114i$. For all cases $n = 0$ and $B = .1$.

$\nu^2\bar{y}_c$ decreases completely shutting down the propagation as $\nu^2 \to 0$ for $\omega = 1$, dimensionless inertial frequency.

Figure 7 shows typical rays in the nondimensional system for the cases for positive and negative $\overline{S}'$ and for ν greater and less than 1. For $\overline{S}' < 0$ we have caustics which are given by (36) where the amplitude becomes unbounded for $D_0^2 + 2\nu^2 \overline{S}'' s = 0$. Of course the field will not be infinite in a real ocean but we would expect larger amplitudes along these caustic lines.

Figure 7 is somewhat misleading because the slopes in the figure must be multiplied by the slope of the front, m, to have a realistic picture. In Figure 8 is a much more realistic geometric representation of the ray field. For typical conditions we see how the field changes as k is increased and the "window" gradually closes. We see that the front is essentially a surface source of internal waves.

We now want to see how well our asymptotic results satisfy the energy balance equation (13). We can construct a composite asymptotic solution for the eigenfunc-

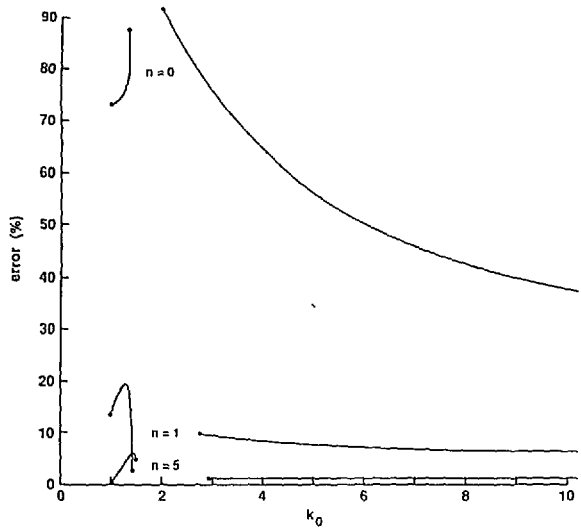

Figure 9. The error in balancing the energy equation (13) integrated over the current layer for $B = .1$ and $k = k_0 + 2n$.

tion h by adding (48), (50) and (54) and subtracting the common parts, (52) and (55). We then integrate (13) numerically over all $y < 0$, using these eigenfunctions.

The accuracy appears to be quite good considering we have a zeroth order solution. As expected the accuracy increases with increasing n and k. This is exemplified in Figure 9 for $B = .1$, where the "error" is the difference of the left and right sides of (13) divided by the left side. We see that the results for $n = 0$ are poor, as expected, but improve dramatically for $n \geq 1$. Calculations for the superinertial instability are more accurate than for the subinertial instability. The accuracy decreases with increasing B, but for $n \geq 5$ we can have $B \simeq 1$ and still have about a 10% error for most values of k.

In general the energy is partitioned almost equally between kinetic and potential. The only difference seen between the superinertial and subinertial instability in the energy equation is the expected difference in the energy flux away from the interface: significant for the former, negligible for the latter.

7. Conclusions

Our canonical front is quite unstable for sufficiently large wavenumber ($> 1/L = f/V_0$). Though the analysis is valid only for small Burger number (B^2), instability for $B = 0(1)$ might be expected since the instability appears to increase with B. However, if the front is viewed as the edge of an eddy or boundary current, we would conclude that these flows are essentially stable since the instability is confined to such a small portion of the flow ($0(V_0/f)$, typically less than 10 km versus 0(100 km)). Even so, the instability is of interest as a local source of internal waves and though the energy loss

from the mean flow due to the internal waves should be relatively small it could be significant in long term evolution of eddies and fronts.

We might speculate on the effect of the instability on the mean flow. Since high wavenumber, high frequency waves are the most unstable and are confined nearest to the vertex of the wedge, we would expect the vertex to be gradually rounded off. This round off would have a horizontal scale of V_0/f and be independent of any viscous effects. Thus we would expect round off even if there is no friction. Would the entire unstable region for all wavenumbers gradually be vertically mixed, erode away and eventually shut off the instability and internal wave production? Linear stability analysis cannot answer this, but the portion of interface which can be unstable which is farthest from the vertex (and eroded away at a slower rate) produces near-inertial waves. Thus we might expect to see a dominance of near-inertial motion beneath the front. This speculation suggests looking to develop a model which takes into account this expected mixing.

Acknowledgments. This work was supported by grant OCE-8915959 from the National Science Foundation.

REFERENCES

Ball F. K. 1963. Some general theorems concerning the finite motion of a shallow rotating liquid lying on a paraboloid. J. Fluid Mech., *17,* 240–256.

Cushman-Roisin, B. 1986a. Frontal geostrophic dynamics. J. Phys. Oceanogr., *16,* 132–143.

—— 1986b. Linear stability of large elliptical warm-core rings. J. Phys. Oceanogr., *16,* 1158–1164.

—— 1987. Exact analytical solutions for elliptical vortices of the shallow-water equations. Tellus, *39A,* 235–244.

Cushman-Roisin, B., W. H. Heil and D. Nof. 1985. Oscillations and rotations of elliptical warm-core rings. J. Geophys. Res., *90,* 11756–11764.

Griffiths, R. W., P. D. Killworth and M. E. Stern. 1982. Ageostrophic instability of ocean currents. J. Fluid Mech., *117,* 343–377.

Hoskins B. J. and F. P. Bretherton. 1972. Atmospheric frontogenesis models: mathematical formulation and solution. J Atm. Sci., *29,* 11–37.

Joyce, T. M. 1984. Velocity and hydrographic structure of a Gulf Stream warm-core ring. J. Phys. Oceanogr., *14,* 936–947.

Killworth, P. D. and M. E. Stern. 1982. Instabilities on density-driven boundary currents and fronts. Geophys. Astrophys. Fluid Dyn., *22,* 1–28.

Kirwan, A. D. and J. Liu. 1989. The shallow water equations on an *f*-plane. Course CIX, "Enrico Fermi School," Nonlinear Topics in Ocean Physics, North Holland.

Kroll, J. 1975. The propagation of wind-generated inertial oscillations from the surface into the deep ocean. J. Mar. Res., *33,* 15–51.

—— 1982. An unstable uniform slab model of the mixed layer as a source of downward propagating near-inertial motion. Part 1: Steady mean flow. J. Mar. Res., *40,* 1013–1033.

—— 1988. Instability of a mixed layer model and the generation of near-inertial motion. Part I: Constant mixed layer depth. J. Phys. Oceanogr., *18,* 963–976.

Lamb, H. 1945. *Hydrodynamics,* 6th ed., Dover Publications, New York.

McWilliams, J. C. and G. R. Flierl. 1976. Optimal, quasi-geostrophic wave analysis of MODE array data. Deep-Sea Res., *23,* 285–300.
Orlanski, I. 1968: Instability of frontal waves. J. Atmos. Sci., *25,* 178–200.
Paldor, N. 1983. Linear stability and stable modes of geostrophic fronts. Geophys. Astrophys. Fluid Dyn., *24,* 299–326.
Ripa, P. 1987. On the stability of elliptical vortex solutions of the shallow-water equations. J. Fluid Mech., *183,* 343–363.
Young, W. R. 1986. Elliptical vortices in shallow water. J. Fluid Mech., *171,* 101–119.

Received: *15 August, 1991;* revised: *3 February, 1992.*